JOURNAL OF GUIDANCE, CONTROL, AND DYNAMICS
Vol. 36, No. 5, September–October 2013

Engineering Notes

Tensor-Product-Model-Based Control of a Three Degrees-of-Freedom Aeroelastic Model

Béla Takarics* and Péter Baranyi†
Hungarian Academy of Sciences, H-1111 Budapest, Hungary

DOI: 10.2514/1.57776

I. Introduction

ACTIVE control of aeroelasticity has been in the focus of aerospace and control engineering for several decades. An introduction to this topic can be found in [1]. This Note largely focuses on the three degrees-of-freedom (DOF) nonlinear aeroelastic test apparatus (NATA) model. The NATA model with unsteady aerodynamics was presented in [2,3] and several active controllers were developed in [4–14]. Linear parameter varying (LPV) control of an improved three DOF aeroelastic model is discussed in [15].

The aim of this Note is to propose a control design strategy to stabilize the improved three DOF NATA model presented in [15], as well as to stabilize the NATA model with nonlinear friction. It is assumed that only the freestream velocity and the pitch angle are measurable, thus an output feedback control structure is applied. The control design considers the following performance requirements: asymptotic stability, decay rate, and constraint on the control signal, which are formulated in terms of linear matrix inequalities (LMIs). The proposed control design strategy has two main steps. First, the quasilinear parameter-varying (qLPV) NATA model is transformed into tensor-product (TP)-type polytopic form via TP model transformation [16–18]. LMI-based control design is applied to the TP-type polytopic form in the second step, which yields a stabilizing controller and observer via optimizing the control performance.

Besides resulting in a stabilizing control solution to the three DOF NATA model, it is shown that the proposed control design methodology has the following properties. The control design can be carried out in a nonheuristic, tractable, and routine-like fashion; the design steps are the same for the three DOF model as for the two DOF model in [9,10]. The model can be extended with additional nonlinearities such as friction. A feasible LMI solution is achieved via convex hull manipulation. The control design strategy is also oblivious as to whether the nonlinearities are given as analytical formulas, in soft-computing form, or as numerical data sets. Numerical simulations are carried out with a perturbed case, in which measurement noise, time delay, parameter uncertainties, and control signal saturation are present.

This Note is structured as follows: Section II presents the equations of motion and the qLPV model of the three DOF aeroelastic wing section. Section III introduces the proposed control design strategy. Based on the control strategy, Sec. IV gives the results of the control design, and Sec. V provides simulation results with evaluation and comparison with results of other published solutions. Conclusions are stated at the end of the Note.

II. Equations of Motion of the Three Degrees-of-Freedom Aeroelastic Wing Section

One of the most recent models of the three DOF aeroelastic wing section based on real measurements, which was adopted in this investigation, was presented and greatly elaborated on in [11,15]. The problem of flutter suppression for the prototypical aeroelastic wing section is considered. The flat plate airfoil is constrained to have three DOF: plunge h, pitch α, and trailing-edge surface deflection β. The equations of motion can be written as

$$\begin{pmatrix} m_h+m_\alpha+m_\beta & m_a x_a b+m_\beta r_\beta+m_\beta x_\beta & m_\beta r_\beta \\ m_a x_a b+m_\beta r_\beta+m_\beta x_\beta & \hat{I}_\alpha+\hat{I}_\beta+m_\beta r_\beta^2+2x_\beta m_\beta r_\beta & \hat{I}_\beta+x_\beta m_\beta r_\beta \\ m_\beta r_\beta & \hat{I}_\beta+x_\beta m_\beta r_\beta & \hat{I}_\beta \end{pmatrix} \begin{pmatrix} \ddot{h} \\ \ddot{\alpha} \\ \ddot{\beta} \end{pmatrix} + \begin{pmatrix} c_h & 0 & 0 \\ 0 & c_\alpha & 0 \\ 0 & 0 & c_{\beta_{\text{servo}}} \end{pmatrix} \begin{pmatrix} \dot{h} \\ \dot{\alpha} \\ \dot{\beta} \end{pmatrix} + \begin{pmatrix} k_h & 0 & 0 \\ 0 & k_\alpha(\alpha) & 0 \\ 0 & 0 & k_{\beta_{\text{servo}}} \end{pmatrix} \begin{pmatrix} h \\ \alpha \\ \beta \end{pmatrix} = \begin{pmatrix} -L \\ M \\ k_{\beta_{\text{servo}}} u_\beta \end{pmatrix} \tag{1}$$

$k_\alpha(\alpha)$ is obtained in [15] by curve fitting on the measured displacement-moment data for a nonlinear spring $k_\alpha(\alpha) = 25.55 - 103.19\alpha + 543.24\alpha^2$. It is important to emphasize that the order of the polynomial defining $k_\alpha(\alpha)$ does not influence the control design methodology (see later). Hence, one can apply a higher-order polynomial to model the nonlinearity of the spring, which can be found in previous works dealing with the aeroelastic wing section model [5].

Quasi-steady aerodynamic force L and moment M are assumed in the same way as earlier works had done in their control design approaches:

$$L = \rho U^2 b C_{l_\alpha}\left(\alpha + \frac{\dot{h}}{U} + \left(\frac{1}{2}-a\right)b\frac{\dot{\alpha}}{U}\right) + \rho U^2 b c_{l_\beta}\beta$$
$$M = \rho U^2 b^2 C_{m_{\alpha,\text{eff.}}}\left(\alpha + \frac{\dot{h}}{U} + \left(\frac{1}{2}-a\right)b\frac{\dot{\alpha}}{U}\right) + \rho U^2 b C_{m_{\beta,\text{eff.}}}\beta \tag{2}$$

The preceding L and M are accurate for the low-velocity regime.

Based on [15], it is assumed that the trailing-edge servomotor dynamics can be represented using a second-order system of the form

$$\hat{I}_\beta\ddot{\beta} + c_{\beta_{\text{servo}}}\dot{\beta} + k_{\beta_{\text{servo}}}\beta = k_{\beta_{\text{servo}}}u_\beta \tag{3}$$

By combining Eqs. (1–3), one obtains

Received 30 January 2012; revision received 5 September 2012; accepted for publication 10 September 2012; published online 5 March 2013.

*Research Fellow, 3D Internet-Based Control and Communications Laboratory, Computer and Automation Research Institute, Kende utca 13-17.
†Head of Laboratory, 3D Internet-Based Control and Communications Laboratory, Computer and Automation Research Institute.

$$\underbrace{\begin{pmatrix} m_h+m_\alpha+m_\beta & m_a x_a b+m_\beta r_\beta+m_\beta x_\beta & m_\beta r_\beta \\ m_a x_a b+m_\beta r_\beta+m_\beta x_\beta & \hat{I}_\alpha+\hat{I}_\beta+m_\beta r_\beta^2+2x_\beta m_\beta r_\beta & \hat{I}_\beta+x_\beta m_\beta r_\beta \\ m_\beta r_\beta & \hat{I}_\beta+x_\beta m_\beta r_\beta & \hat{I}_\beta \end{pmatrix}}_{\mathbf{M}_{\text{eom}}} \times \begin{pmatrix} \ddot{h} \\ \ddot{\alpha} \\ \ddot{\beta} \end{pmatrix} + \underbrace{\begin{pmatrix} c_h+\rho b S C_{l_\alpha} U & \left(\frac{1}{2}-a\right) b\rho b S C_{l_\alpha} U & 0 \\ -\rho b^2 S C_{m_{\alpha,\text{eff}}} U & c_\alpha-\left(\frac{1}{2}-a\right) b\rho b^2 S C_{m_{\alpha,\text{eff}}} U & 0 \\ 0 & 0 & c_{\beta_{\text{servo}}} \end{pmatrix}}_{\mathbf{C}_{\text{eom}}} \begin{pmatrix} \dot{h} \\ \dot{\alpha} \\ \dot{\beta} \end{pmatrix}$$

$$+ \underbrace{\begin{pmatrix} k_h & \rho b S C_{l_\alpha} U^2 & \rho b S C_{l_\beta} U^2 \\ 0 & k_\alpha(\alpha)-\rho b^2 S C_{m_{\alpha,\text{eff}}} U^2 & -\rho b^2 S C_{m_{\beta,\text{eff}}} U^2 \\ 0 & 0 & k_{\beta_{\text{servo}}} \end{pmatrix}}_{\mathbf{K}_{\text{eom}}} \begin{pmatrix} h \\ \alpha \\ \beta \end{pmatrix} = \underbrace{\begin{pmatrix} 0 \\ 0 \\ k_{\beta_{\text{servo}}} \end{pmatrix}}_{\mathbf{F}_{\text{eom}}} \mathbf{u} \tag{4}$$

where $\mathbf{M}_{\text{eom}}$, $\mathbf{C}_{\text{eom}}$, $\mathbf{K}_{\text{eom}}$, and $\mathbf{F}_{\text{eom}}$ are the mass, damping, stiffness, and forcing matrices of the equation of motion [15].

The preceding equation can be transformed to the state-space qLPV form of

$$\begin{pmatrix} \dot{\mathbf{x}}(t) \\ \mathbf{y}(t) \end{pmatrix} = \mathbf{S}(\mathbf{p}(t)) \begin{pmatrix} \mathbf{x}(t) \\ \mathbf{u}(t) \end{pmatrix} \tag{5}$$

with input $\mathbf{u}(t) = u_\beta \in \mathbb{R}$, the measurable output $\mathbf{y}(t) = \alpha \in \mathbb{R}$, and state vector

$$\mathbf{x}(t) = (\,\mathbf{x}_1(t) \quad \mathbf{x}_2(t) \quad \mathbf{x}_3(t) \quad \mathbf{x}_4(t) \quad \mathbf{x}_5(t) \quad \mathbf{x}_6(t)\,)^T = (\,\dot{h} \quad \dot{\alpha} \quad \dot{\beta} \quad h \quad \alpha \quad \beta\,)^T \in \mathbb{R}^6$$

The system matrix

$$\mathbf{S}(\mathbf{p}(t)) = \begin{pmatrix} \mathbf{A}(\mathbf{p}(t)) & \mathbf{B}(\mathbf{p}(t)) \\ \mathbf{C}(\mathbf{p}(t)) & \mathbf{D}(\mathbf{p}(t)) \end{pmatrix} \in \mathbb{R}^{7\times 7} \tag{6}$$

is a parameter-varying object, where $\mathbf{p}(t) = (\,U(t) \quad \alpha(t)\,)^T \in \Omega$ and $\Omega = [a_1, b_1] \times [a_2, b_2]$ is a closed hypercube. Since $\mathbf{p}(t)$ includes α, an element of $\mathbf{x}(t)$, Eq. (6) belongs to the class of qLPV systems.

The elements of $\mathbf{S}(\mathbf{p}(t))$ are

$$\mathbf{A}(\mathbf{p}(t)) = \begin{pmatrix} -\mathbf{M}_{\text{eom}}^{-1}\mathbf{C}_{\text{eom}}(\mathbf{p}(t)) & -\mathbf{M}_{\text{eom}}^{-1}\mathbf{K}_{\text{eom}}(\mathbf{p}(t)) \\ -\mathbf{I} & 0 \end{pmatrix},$$

$$\mathbf{B} = \begin{pmatrix} \mathbf{M}_{\text{eom}}^{-1}\mathbf{F}_{\text{eom}} \\ 0 \end{pmatrix} \quad \mathbf{C} = (\,0 \quad 0 \quad 0 \quad 0 \quad 1 \quad 0\,) \quad \text{and} \quad \mathbf{D} = 0 \tag{7}$$

The details and definition of each system parameter can be found in [15] and they have the following values:

$m_h = 6.516$ kg; $m_\alpha = 6.7$ kg; $m_\beta = 0.537$ kg; $x_\alpha = 0.21$; $x_\beta = 0.233$; $r_\beta = 0$ m; $a = -0.673$ m; $b = 0.1905$ m; $\hat{I}_\alpha = 0.126$ kgm^2; $\hat{I}_\beta = 10^{-5}$; $c_h = 27.43$ Nms/rad; $c_\alpha = 0.215$ Nms/rad; $c_{\beta_{\text{servo}}} = 4.182 * 10^{-4}$ Nms/rad; $k_h = 2844$; $k_{\beta_{\text{servo}}} = 7.6608 * 10^{-3}$; $\rho = 1.225$ kg/m^3; $C_{l_\alpha} = 6.757$; $C_{m_{\alpha,\text{eff}}} = -1.17$; $C_{l_\beta} = 3.774$; $C_{m_{\beta,\text{eff}}} = -2.1$; and $S = 0.5945$ m.

III. Proposed Control Design Strategy

A. Reconstruction of the Tensor-Product-Type Polytopic Model

The mathematical background of the TP model transformation and TP model transformation-based LMI control design was introduced and elaborated on in [16–18] and the methodology was presented in [9,10] for the two DOF aeroelastic model. The main definitions related to TP model transformation and TP-type polytopic models are as follows.

Definition 1 [finite element TP-type polytopic model (TP model)]: $\mathbf{S}(\mathbf{p}(t))$ in Eq. (6) is given for any parameter as the parameter-varying convex combination of LTI system matrices $\mathbf{S} \in \mathbb{R}^{O\times I}$:

$$\mathbf{S}(\mathbf{p}(t)) = \sum_{i_1=1}^{I_1}\sum_{i_2=1}^{I_2}\cdots\sum_{i_N=1}^{I_N} w_{n,i_n}(p_n(t))\mathbf{S}_{i_1,i_2,\ldots,i_N} = \mathcal{S}\boxtimes_{n=1}^{N}\mathbf{w}_n(p_n(t)) \tag{8}$$

where $\mathbf{p}(t) \in \Omega$. The $(N+2)$-dimensional coefficient tensor $\mathcal{S} \in \mathbb{R}^{I_1\times I_2\times\ldots\times I_n\times O\times I}$ is constructed from the LTI vertex systems $\mathbf{S}_{i_1,i_2,\ldots,i_N}$ (8) and the row vector $\mathbf{w}_n(p_n(t))$ contains one variable and continuous weighting functions $w_{n,i_n}(p_n(t))$, $i_n = 1 \ldots I_N$. The weighting functions satisfy the following criteria:

$$\forall\, n, i, p_n(t)\colon\ w_{n,i}(p_n(t)) \in [0,1] \tag{9}$$

$$\forall\, n, p_n(t)\colon\ \sum_{i=1}^{I_n} w_{n,i}(p_n(t)) = 1 \tag{10}$$

Definition 2 [normal/close to normal (NO/CNO), normal-type TP model]: The TP model is a NO-type model if its weighting functions are normal, that is, if it satisfies Eqs. (9) and (10), and the largest value of all weighting functions is one. The convex TP model is CNO if it satisfies Eqs. (9) and (10), and the largest value of all weighting functions is one or close to one.

Definition 3 (TP model transformation): TP model transformation is a numerical method to transform qLPV models given in the form of Eq. (6) to a TP-type polytopic model in the form of Eq. (8), so that a large class of LMI-based control design techniques can be immediately applied. If the original qLPV model has no exact TP representation, TP model transformation is capable of finding the TP-type approximants of arbitrary accuracy. This feature can also be useful for complexity reduction via finding the best lower rank approximation in the $\mathcal{L}_2$ sense.

TP model transformation can be executed uniformly (irrespective of whether the model is given in the form of analytical equations resulting from physical considerations or as an outcome of soft-computing-based identification techniques, such as neural networks or fuzzy-logic-based methods, or as a result of a black-box identification, etc.), within a reasonable amount of time [17]. Thus, the transformation replaces the analytical and, in many cases, complex and not obvious conversions to numerical, tractable, and straightforward operations that can be carried out in a routine fashion.

B. Control Structure

A large class of LMI-based control design techniques is available for polytopic models. The control design technique applied in this research results in a controller and observer, which have the polytopic of the model. It is assumed that not all of the state variables of the NATA model are measurable (in the present research, only the pitch angle α is measurable); therefore, output feedback design structure is applied. The observers are required to satisfy $\mathbf{x}(t) - \hat{\mathbf{x}}(t) \to 0$ as $t \to \infty$, where $\hat{\mathbf{x}}(t)$ denotes the state vector estimated by the observer. Since $\mathbf{p}(t)$ does not contain values from the estimated state vector $\hat{\mathbf{x}}(t)$, thus the following strategy for controller and observed design was used [19,20]:

$$\dot{\hat{\mathbf{x}}}(t) = \mathbf{A}(\mathbf{p}(t))\hat{\mathbf{x}}(t) + \mathbf{B}(\mathbf{p}(t))\mathbf{u}(t) + \mathbf{K}(\mathbf{p}(t))(\mathbf{y}(t) - \hat{\mathbf{y}}(t))$$
$$\hat{\mathbf{y}}(t) = \mathbf{C}(\mathbf{p}(t))\hat{\mathbf{x}}(t)$$

where $\mathbf{u}(t) = -\mathbf{F}(\mathbf{p}(t))\mathbf{x}(t)$. This takes the following TP-type polytopic structure:

$$\begin{aligned}\dot{\hat{\mathbf{x}}}(t) &= \mathcal{A} \overset{N}{\underset{n=1}{\boxtimes}} \mathbf{w}_n(p_n(t))\hat{\mathbf{x}}(t) + \mathcal{B} \overset{N}{\underset{n=1}{\boxtimes}} \mathbf{w}_n(p_n(t))\mathbf{u}(t) \\ &\quad + \mathcal{K} \overset{N}{\underset{n=1}{\boxtimes}} \mathbf{w}_n(p_n(t))(\mathbf{y}(t) - \hat{\mathbf{y}}(t)) \\ \hat{\mathbf{y}}(t) &= \mathcal{C} \overset{N}{\underset{n=1}{\boxtimes}} \mathbf{w}_n(p_n(t))\hat{\mathbf{x}}(t) \\ \mathbf{u}(t) &= -(\mathcal{F} \overset{N}{\underset{n=1}{\boxtimes}} \mathbf{w}_n(p_n(t)))\mathbf{x}(t) \end{aligned} \tag{11}$$

The goal of the design is to determine gains $\mathcal{F}$ and $\mathcal{K}$ in such a way that the stability of the output-feedback control structure is guaranteed. The linear time-invariant (LTI) feedback gains $\mathbf{F}_{i_1,i_2,\ldots,i_N}$ and observer gains $\mathbf{K}_{i_1,i_2,\ldots,i_N}$ stored in tensor $\mathcal{F}$ and $\mathcal{K}$ are called vertex feedback gains and vertex observer gains, respectively.

C. Control Performance Optimization Based on Linear Matrix Inequalities

There are several LMI theorems available for observer and controller design to derive the vertex gains $\mathcal{K}$ of the observer and the feedback gains $\mathcal{F}$ of the controller.

The following control performance requirements were specified: 1) asymptotic stability for the controller and observer; 2) decay rate for the controller; and 3) constrain on the control value for the controller.

This Note selects the same LMI theorems as applied for the 2 DOF aeroelastic wing case presented in [9,10]:

Theorem 1 (globally and asymptotically stable observer and controller): Assume the polytopic model (8) with controller and observer structure (11). This output-feedback control structure is globally and asymptotically stable if there exists such $\mathbf{P}_1 > 0, \mathbf{P}_2 > 0$ and $\mathbf{M}_{1,r}$, $\mathbf{N}_{2,r}$ ($r = 1, \ldots, R$ and R is the number of LTI vertex systems) satisfying equations

$$\begin{aligned}&\mathbf{P}_1\mathbf{A}_r^T - \mathbf{M}_{1,r}^T\mathbf{B}_r^T + \mathbf{A}_r\mathbf{P}_1 - \mathbf{B}_r\mathbf{M}_{1,r} < \mathbf{0}, \\ &\mathbf{A}_r^T\mathbf{P}_2 - \mathbf{C}_r^T\mathbf{N}_{2,r}^T + \mathbf{P}_2\mathbf{A}_r - \mathbf{N}_{2,r}\mathbf{C}_r < \mathbf{0}, \\ &\mathbf{P}_1\mathbf{A}_r^T - \mathbf{M}_{1,s}^T\mathbf{B}_r^T + \mathbf{A}_s\mathbf{P}_1 - \mathbf{B}_r\mathbf{M}_{1,s} + \mathbf{P}_1\mathbf{A}_s^T - \mathbf{M}_{1,r}^T\mathbf{B}_s^T \\ &\quad + \mathbf{A}_s\mathbf{P}_1 - \mathbf{B}_s\mathbf{M}_{1,r} < \mathbf{0}, \\ &\mathbf{A}_r^T\mathbf{P}_2 - \mathbf{C}_s^T\mathbf{N}_{2,r}^T + \mathbf{P}_2\mathbf{A}_r - \mathbf{N}_{2,r}\mathbf{C}_s + \mathbf{A}_s^T\mathbf{P}_2 - \mathbf{C}_r^T\mathbf{N}_{2,s}^T \\ &\quad + \mathbf{P}_2\mathbf{A}_s - \mathbf{N}_{2,s}\mathbf{C}_r < \mathbf{0}\end{aligned}$$

for $r < s \le R$, except the pairs (r, s) such that $\forall \mathbf{p}(t)$: $w_r(\mathbf{p}(t))w_s(\mathbf{p}(t)) = 0$, and where $\mathbf{M}_{1,r} = \mathbf{F}_r\mathbf{P}_1$ and $\mathbf{N}_{2,r} = \mathbf{P}_2\mathbf{K}_r$. The feedback and observer gains can then be obtained from the solution of the preceding LMIs as $\mathbf{F}_r = \mathbf{M}_{1,r}\mathbf{P}_1^{-1}$ and $\mathbf{K}_r = \mathbf{P}_2^{-1}\mathbf{N}_{2,r}$.

Theorem 2 (globally and asymptotically stable observer and controller with decay rate):

$$\begin{aligned}&\mathbf{P}_1\mathbf{A}_r^T - \mathbf{M}_{1,r}^T\mathbf{B}_r^T + \mathbf{A}_r\mathbf{P}_1 - \mathbf{B}_r\mathbf{M}_{1,r} + 2\alpha\mathbf{P}_1 < \mathbf{0}, \\ &\mathbf{A}_r^T\mathbf{P}_2 - \mathbf{C}_r^T\mathbf{N}_{2,r}^T + \mathbf{P}_2\mathbf{A}_r - \mathbf{N}_{2,r}\mathbf{C}_r + 2\alpha\mathbf{P}_2 < \mathbf{0}, \\ &\mathbf{P}_1\mathbf{A}_r^T - \mathbf{B}_s\mathbf{M}_{1,r} - \mathbf{M}_{1,s}^T\mathbf{B}_r^T + \mathbf{A}_s\mathbf{P}_1 - \mathbf{B}_r\mathbf{M}_{1,s} + \mathbf{P}_1\mathbf{A}_s^T \\ &\quad - \mathbf{M}_{1,r}^T\mathbf{B}_s^T + \mathbf{A}_s\mathbf{P}_1 + 4\alpha\mathbf{P}_1 < \mathbf{0}, \\ &\mathbf{A}_r^T\mathbf{P}_2 - \mathbf{C}_s^T\mathbf{N}_{2,r}^T + \mathbf{P}_2\mathbf{A}_r - \mathbf{N}_{2,r}\mathbf{C}_s + \mathbf{A}_s^T\mathbf{P}_2 - \mathbf{C}_r^T\mathbf{N}_{2,s}^T \\ &\quad + \mathbf{P}_2\mathbf{A}_s - \mathbf{N}_{2,s}\mathbf{C}_r + 4\alpha\mathbf{P}_2 < \mathbf{0},\end{aligned}$$

Solving the LMIs yields an asymptotically stable observer and controller with decay rate.

Theorem 3 (globally and asymptotically stable observer and controller with constraint on the control value): Simultaneously solving the LMIs of Theorem 1 with Theorem 3 in the form of

$$\phi^2\mathbf{I} \le \mathbf{P}_1 \quad \begin{pmatrix} \mathbf{P}_1 & \mathbf{M}_r^T \\ \mathbf{M}_r & \mu^2\mathbf{I} \end{pmatrix} \ge 0$$

leads to an asymptotically stable controller and observer structure with bounded l_2 norm of the controller.

One can utilize or design further LMIs to guarantee various additional constraints.

D. Searching Feasibility of Linear Matrix Inequality Tests via Convex Hull Manipulation

LMI-based design yields an optimized solution for the given convex hull, rather than for the given qLPV problem, making the control design conservative. As such, the feasibility test of LMIs is sensitive to the actual polytopic form of the model [21], hence both the LMI-based optimization and the convex hull manipulation must be simultaneously investigated for control system design. A number of different convex models were defined in [10]. Sum Normalized Non-Negative (SNNN)-, CNO- and Inverted and Relaxed Normal (IRNO)-type convex representations were examined in the current investigation, however, only the CNO-type representation was able to lead to a feasible LMI solution (see later).

IV. Results of the Control Design

A. Tensor Produce Model of the Three Degrees-of-Freedom Aeroelastic Wing Section

TP model transformation (generating CNO-type weighting functions) is executed on the qLPV state-space model (7). The transformation space Ω is defined in the interval $U \in [8, 20]$ m/s and $\alpha \in [-0.3, 0.3]$ rad and the grid density is defined as $M_1 \times M_2$, $M_1 = 137$, and $M_2 = 137$. TP model transformation results in the rank of the discretized tensor $\mathcal{S}^D \in \mathbb{R}^{M_1 \times M_2 \times 6 \times 6}$, which is two in the first dimension and three in the second dimension. The weighting functions $w_{1,i}(U)$, $i = 1 \ldots 2$, and $w_{2,j}(\alpha)$, $j = 1 \ldots 3$, are depicted in Fig. 1. The aeroelastic model (7) can be transformed exactly to finite element TP-type polytopic model form with six vertex LTI models.

B. Linear Matrix Inequality-Based Output Feedback Controller Design

LMI-based control design can be immediately applied to the TP-type polytopic form of the aeroelastic model (7) and the following controllers were designed.

1. *Controller 1: Asymptotic Stabilization and Decay Rate Control*

By applying Theorem 2, one finds that $\alpha = 0$ gives the best controller performance for the present model. This simply means that the LMIs in Theorem 2 become equivalent to the LMIs of Theorem 1.

2. *Controller 2: Constraint on the Control Value*

Two additional control solutions are also designed. To limit the bounds of the control values, Theorem 3 was applied. The minimal l_2 bound of the control value that still guarantees feasible LMIs was searched in the case of controller 2.1 "min". For comparison, controller 2.2 "max" was also derived, where a 10 times larger bound limit of the control signal was applied.

C. Controller 3: Asymptotic State Feedback Control of the Nonlinear Aeroelastic Test Apparatus Model with Nonlinear Friction

The damping of the aeroelastic wing model in Eq. (3) has a linear viscous term. However, in many cases, nonlinear friction models give a more realistic description of the physical phenomenon, thus the linear viscous term is replaced by a Stribeck friction model in the

present section. Simulation results showed that the previously designed controllers are not able to stabilize the NATA model with Stribeck friction. This comes from the fact that dimension of the nonlinearity increased. The aim of controller 3 is to show how a given qLPV model can be extended with additional nonlinearities and how the controller can be derived systematically in a routine-like manner by applying the proposed control design strategy.

A Stribeck friction model defined in the following form is applied:

$$F_f(t) = -\left(F_c + \frac{(F_s - F_c)}{\left(1 + \left(\frac{v}{v_s}\right)^2\right)}\right)\text{sign}(v(t)) - F_v v \qquad (12)$$

where $c_{\beta_{\text{servoC}}} = 4.182 * 10^{-}4$ Nm is the Coulomb friction term, $c_{\beta_{\text{servoS}}} = 1.2 \cdot c_{\beta_{\text{servoC}}}$ is the Stribeck friction term, and $\dot{\beta}_{\text{Stribeck}} = 0.0075$ rad/s is the Stribeck velocity. The values of these parameters were chosen based on engineering considerations to obtain a realistic friction model. It must be mentioned that other nonlinear friction models can also be implemented, which can be given in analytical, soft-computing form, or as data sets.

The parameter space Ω has to be extended by one dimension in $x_3(t) = \dot{\beta}$. The friction model is expected to be valid in the interval of $\dot{\beta} \in [-1.5, 1.5]$ rad/s. The grid density can be defined as $M_1 \times M_2 \times M_3$, $M_1 = 137$, $M_2 = 137$, and $M_2 = 138$ (an even number for the grid in the third dimension is chosen to avoid division by zero during discretization). The TP model transformation results in a CNO-type TP polytopic model, the rank of the discretized tensor $\mathcal{S}^D \in \mathbb{R}^{M_1 \times M_2 \times M_3 \times 6 \times 6}$ is 2, 3, 2 in the first, second, and third dimensions, respectively. The number of vertexes becomes $2 \times 3 \times 2 = 12$. The weighting functions can be seen in Fig. 1.

State feedback controller 3 for the preceding model was designed by applying the controller related terms of Theorem 1.

V. Numerical Experiment Results and Evaluation

A. Simulation

Numerical experiments are presented to demonstrate the performance of the designed stabilizing control solution. Freestream velocity and $U = 14.1$ m/s is chosen to be comparable to other published results. Open-loop simulation was performed at the beginning of each test to let the oscillations fully develop. However, in the resulting figures, only the range of the simulation is shown where the controller is on.

Two simulation cases were compared for each controller.

1) Case 1: A perturbed system is used to test the robustness of the solution. Case 1 includes random noise normally distributed with a variance of 10% added to the measured output signal; 3 ms constant time delay representing the computational delay; modified nominal values of masses and inertia by $\pm 15\%$; and saturation of the control value.

2) Case 2: An ideal reference case represents the ideal simulation cases without the perturbations listed in case 1.

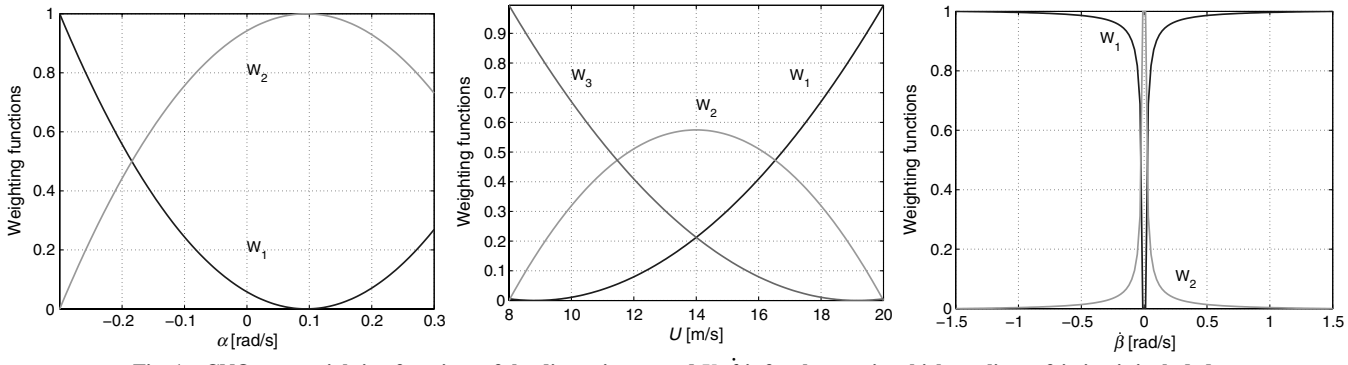

Fig. 1 CNO-type weighting functions of the dimensions α and U; $\dot{\beta}$ is for the case in which nonlinear friction is included.

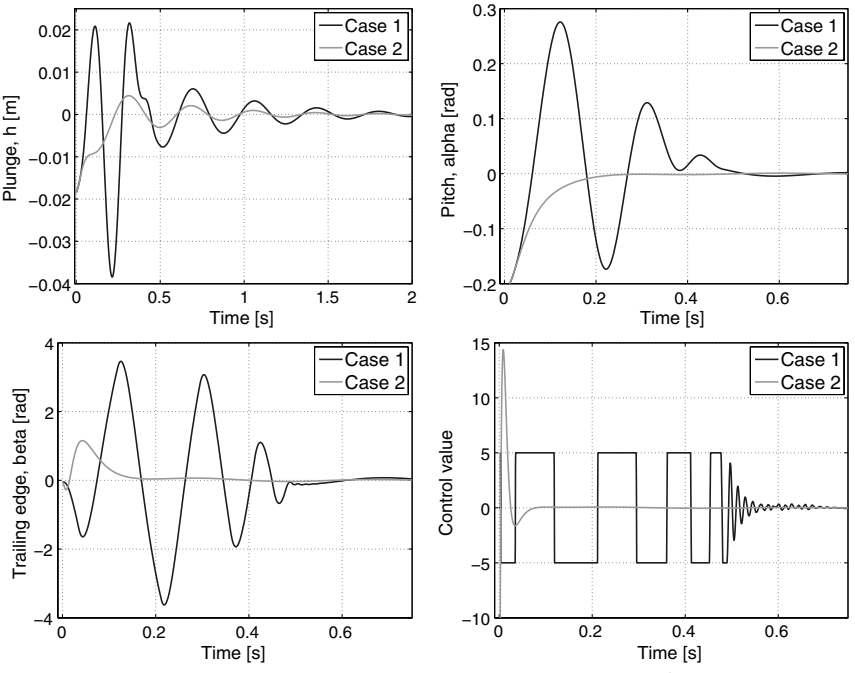

Fig. 2 Time response of controller 2.1 for $U = 14.1$ m/s.

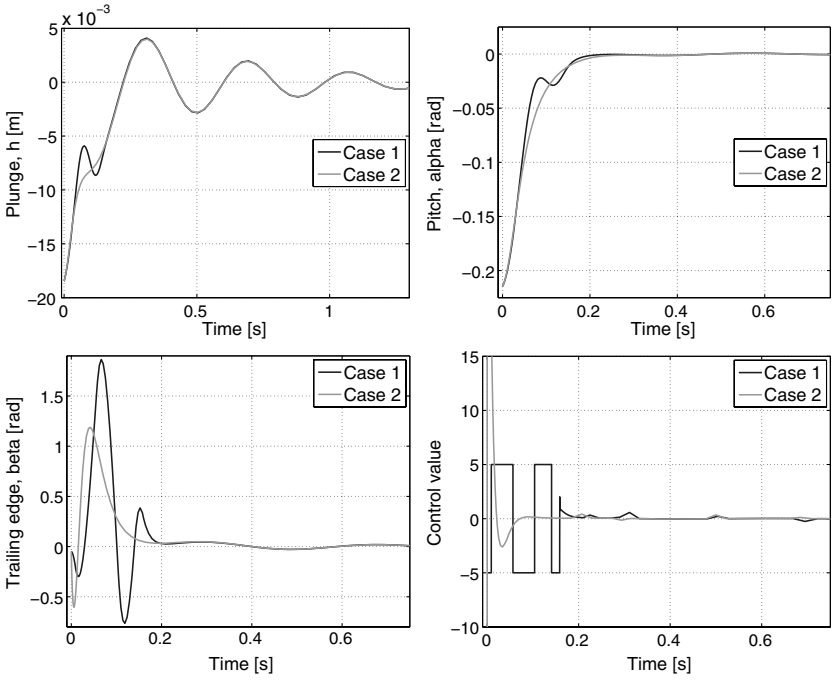

Fig. 3 Time response of controller 3 for $U = 14.1$ m/s.

In the case of controller 3, the case 1 simulation has saturation of the control signal as the only perturbation.

Figures 2 and 3 show the time response of the controlled system for controllers 2.1 and 3, respectively.

Simulation for controller 2.1 with sinusoidally varying freestream velocity are also performed; the results can be seen in Fig. 4.

B. Evaluation

All of the designed controllers are able to asymptotically stabilize the state variables of the NATA model with linear and nonlinear friction. Controller 2.1 out of controllers 1, 2.1, and 2.2 has the smallest control signal amplitude in case 2 and desaturates in 0.5 s, whereas the others desaturate in 0.9 s in case 1. The settling times are similar for all of the controllers. Thus, it can be concluded that controller 2.1 has the most favorable properties, therefore the simulation results of controller 2.1 are given in Fig. 2.

1. Stability

An important issue should be addressed here. The applied LMIs guarantee that the resulting controller is stable. However, the TP model transformation is a numerical method that can be performed over an arbitrarily, but bounded domain Ω. Therefore, the stability ensured by the applied LMIs is restricted to Ω. Note that the accuracy of the given model is also bounded in reality for low speeds. The resulting controllers guarantee asymptotic stability in Ω: $[-0.3, 0.3] \times [8, 20]$. One may extend Ω and execute the

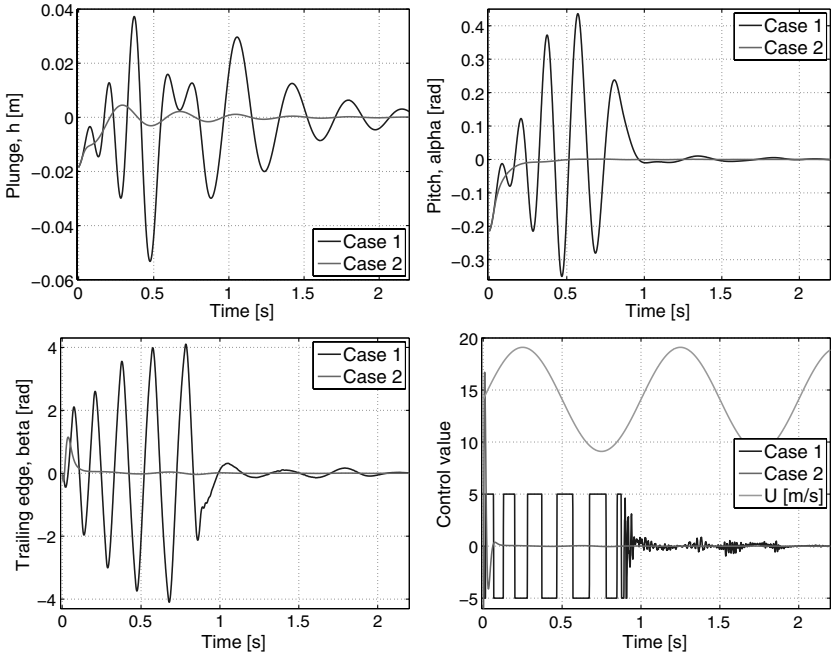

Fig. 4 Time response of controller 2.1 with sinusoidally varying freestream velocity.

Table 1 Maximal control values and the settling times for the designed control solutions

	Maximal control value	Settling time, s
Controller 1.1	Case 1: 5; case 2: −350	Case 1: 1.5; case 2: 1.5
Controller 2.1	Case 1: 5; case 2: −15	Case 1: 1.5; case 2: 1
Controller 2.2	Case 1: 5; case 2: −60	Case 1: 1.5; case 2: 1
Controller 3	Case 1: 5; case 2: −14, 500	Case 1: 1.5; case 2: 1.5

design method again. Controller 3 has an additional dimension in domain Ω, thus the stability domain becomes Ω: $[-0.3, 0.3] \times [8, 20] \times [-1.5, 1.5]$.

2. Performance Discussion

The control performance discussion focuses on two objectives based on the control performance specifications given previously. These are the maximal control values and the settling time for each controller. The evaluation is summarized in Table 1.

It can be concluded that controller 2.1 out of the first three designed controllers has the best performance according to our objectives. Controller 3 has a performance that is similar to controller 1. However, controller 3 has to stabilize the system with an additional nonlinearity caused by the friction.

3. Comparison with Other Results Found in Recent Technical Literature

a. Control Performance—The control performance can be compared with the results presented in [15], where the linear quadratic regulator (LQR) controller was designed for the same three DOF aeroelastic wing sections. One can observe that the controllers derived with the TP-type polytopic model and LMI design produce considerably faster responses in case 2, but the cost is a higher control value. Case 1, which is a more realistic physical environment, saturates the control signal, making the settling time somewhat longer, comparable with the results found in [15]. It also has to be mentioned that the LPV model in [15] has nonlinearity only in one dimension, namely in U, and the controller designed in the same paper is not output, but a full state feedback controller.

A similar model was examined in [22], in which an LQR-based output feedback controller was designed. The control performance is similar to the performance of controller 2.1. However, simulation case 1 of controller 2.1 also includes time delay, parameter uncertainties, and noise on the measured output signal.

The control performance, based on the aforementioned criteria, is similar to the controller presented in [9], which can be expected, because the same LMIs and control design methodology were used. On the other hand, it has to be emphasized that the present controller is designed for the three DOF model, rather than the two DOF model, and the results of case 1 simulations include time delay, noise on the measured signal, control signal saturation, and parameter uncertainties.

Multi-input/multi-output control designs are used in [8,12,23]. However, the actuator dynamics are not included in the models in those cases.

b. Control Design Methodology—Note that very simple LMI theorems have been applied so far. If one would like to go for higher control performance, various choices of performance specifications could be attempted through more powerful LMI design theorems and further convex hull manipulation. Former solutions of the three DOF aeroelastic control problem do not focus on considerations other than stability.

VI. Conclusions

The proposed numerical control design methodology for tensor-product-type polytopic models can be executed systematically in a routine-like manner and preserves this property even if the model is extended with additional nonlinearities (such as friction). The proposed methodology is capable of control performance optimization through the use of linear matrix inequalities and convex hull manipulation. Based on the proposed control design methodology, this Note gives a stabilizing control solution for the three degree-of-freedom aeroelastic wing section with linear and nonlinear friction. It is shown by simulation of a perturbed model that the designed controller and observer are resilient to a variety of perturbations. The next step of the research is to design a stabilizing control solution to the same wing model with parameter uncertainties and the time delay included in the design phase and in the model, and thus guarantees on the robustness can be made.

Acknowledgments

The research was supported by the National Research and Technology Agency, (ERC_09) (OMFB-01677/2009) (ERC-HU-09-1-2009-0004 MTA SZTAK), and Control Research Group of Hungarian Academy of Science.

References

[1] Mukhopadhyay, V., "Historical Perspective on Analysis and Control of Aeroelastic Responses," *Journal of Guidance, Control, and Dynamics*, Vol. 26, No. 5, 2003, pp. 673–684. doi:10.2514/2.5108

[2] Block, J. J., and Gilliat, H., "Active Control of an Aeroelastic Structure," *AIAA Meeting Papers on Disc*, AIAA, Reston, VA, Jan. 1997, pp. 1–11; also Paper 1997-16.

[3] Block, J. J., and Strganac, T. W., "Applied Active Control for a Nonlinear Aeroelastic Structure," *Journal of Guidance, Control, and Dynamics*, Vol. 21, No. 6, 1998, pp. 838–845. doi:10.2514/2.4346

[4] Mukhopadhyay, V., "Transonic Flutter Suppression Control Law Design and Wind-Tunnel Test Results," *Journal of Guidance, Control, and Dynamics*, Vol. 23, No. 5, Sept. 2000, pp. 930–937. doi:10.2514/2.4635

[5] Strganac, T. W., Ko, J., and Thompson, D. E., "Identification and Control of Limit Cycle Oscillations in Aeroelastic Systems," *Journal of Guidance, Control, and Dynamics*, Vol. 23, No. 6, 2000, pp. 1127–1133. doi:10.2514/2.4664

[6] Singh, S. N., and Wang, L., "Output Feedback Form and Adaptive Stabilization of a Nonlinear Aeroelastic System," *Journal of Guidance, Control, and Dynamics*, Vol. 25, No. 4, July 2002, pp. 725–732. doi:10.2514/2.4939

[7] Platanitis, G., and Strganac, T., "Suppression of Control Reversal Using Leading- and Trailing-Edge Control Surfaces," *Journal of Guidance, Control, and Dynamics*, Vol. 28, No. 3, 2005, pp. 452–460. doi:10.2514/1.6692

[8] Reddy, K. K., Chen, J., Behal, A., and Marzocca, P., "Multi-Input/Multi-Output Adaptive Output Feedback Control Design for Aeroelastic Vibration Suppression," *Journal of Guidance, Control, and Dynamics*, Vol. 30, No. 4, 2007, pp. 1040–1048. doi:10.2514/1.27684

[9] Baranyi, P., "Tensor Product Model-Based Control of Two-Dimensional Aeroelastic System," *Journal of Guidance, Control, and Dynamics*, Vol. 29, No. 2, March 2006, pp. 391–400. doi:10.2514/1.9462

[10] Baranyi, P., "Output Feedback Control of Two-Dimensional Aeroelastic System," *Journal of Guidance, Control, and Dynamics*, Vol. 29, No. 3, May 2006, pp. 762–767. doi:10.2514/1.14981

[11] Prime, Z., Cazzolato, B., and Doolan, C., "A Mixed H_2/H_∞ Scheduling Control Scheme for a Two Degree-Of-Freedom Aeroelastic System Under Varying Airspeed and Gust Conditions," *Proceedings of the AIAA Guidance, Navigation and Control Conference and Exhibit*, Curran Associates, Inc., New York, NY, 2008; also Paper 2008-6787.

[12] Lee, K. W., and Singh, S. N., "Multi-Input Noncertainty-Equivalent Adaptive Control of an Aeroelastic System," *Journal of Guidance, Control, and Dynamics*, Vol. 33, Sept. 2010, pp. 1451–1460. doi:10.2514/1.48302

[13] Grof, P., Baranyi, P., and Korondi, P., "Convex Hull Manipulation Based Control Performance Optimisation," *WSEAS Transactions on Systems and Control*, Vol. 5, No. 8, Aug. 2010, pp. 691–700.

[14] Takarics, B., Grof, P., Baranyi, P., and Korondi, P., *Friction Compensation of an Aeroelastic Wing — A TP Model Transformation Based Approach*, IEEE Publ., Piscataway, NJ, Sept. 2010, pp. 527–533.

[15] Prime, Z., Cazzolato, B., Doolan, C., and Strganac, T., "Linear-Parameter-Varying Control of an Improved Three-Degree-of-Freedom

Aeroelastic Model," *Journal of Guidance, Control, and Dynamics*, Vol. 33, No. 2, 2010, pp. 615–618.
doi:10.2514/1.45657

[16] Baranyi, P., Szeidl, L., Várlaki, P., and Yam, Y., "Definition of the HOSVD-Based Canonical Form of Polytopic Dynamic Models," *Third International Conference on Mechatronics (ICM 2006)*, Inst. of Electrical and Electronics Engineers (IEEE), New York, NY, July 2006, pp. 660–665.

[17] Baranyi, P., "TP Model Transformation as a Way to LMI Based Controller Design," *IEEE Transactions on Industrial Electronics*, Vol. 51, No. 2, 2004, pp. 387–400.
doi:10.1109/TIE.2003.822037

[18] Baranyi, P., Szeidl, L., Várlaki, P., and Yam, Y., "Numerical Reconstruction of the HOSVD-Based Canonical Form of Polytopic Dynamic Models," *10th International Conference on Intelligent Engineering Systems*, Inst. of Electrical and Electronics Engineers (IEEE), New York, NY, June 2006, pp. 196–201.

[19] Scherer, C. W., and Weiland, S., *Linear Matrix Inequalities in Control*, DISC Course Lecture Notes, 2000, http://w3.ele.tue.nl/fileadmin/ele/MBS/CS/Files/Courses/DISClmi/lmis1.pdf [retrieved 5 Feb. 2012].

[20] Tanaka, K., and Wang, H. O., *Fuzzy Control Systems Design and Analysis: A Linear Matrix Inequality Approach*, Wiley, New York, 2001, pp. 83–90.

[21] Baranyi, P., "Convex Hull Generation Methods for Polytopic Representations of LPV Models," *Seventh International Symposium on Applied Machine Intelligence and Informatics (SAMI 2009)*, Inst. of Electrical and Electronics Engineers (IEEE), New York, NY, Jan. 2009, pp. 69–74.

[22] Bhoir, N., "Output Feedback Nonlinear Control of an Aeroelastic System with Unsteady Aerodynamics," *Aerospace Science and Technology*, Vol. 8, No. 4, 2004, pp. 195–205.
doi:10.1016/j.ast.2003.10.009

[23] Wang, Z., Behal, A., and Marzocca, P., "Model-Free Control Design for Multi-Input Multi-Output Aeroelastic System Subject to External Disturbance," *Journal of Guidance, Control, and Dynamics*, Vol. 34, No. 2, March 2011, pp. 446–458.
doi:10.2514/1.51403